Research in Pharmaceutical Sciences, February 2023; 18(1): 24-38
Received: 13-08-2022
Peer Reviewed: 22-08-2022
Revised: 04-09-2022
Accepted: 11-09-2022
Published: 24-12-2022

School of Pharmacy & Pharmaceutical Sciences
Isfahan University of Medical Sciences

Original Article

Synthesis of oxamide-hydrazone hybrid derivatives as potential anticancer agents

Mina Dehbid[1], Raheleh Tahmasvand[2], Marzieh Tasharofi[3], Fatemeh Shojaie[3], Mahmoudreza Aghamaali[1], Ali Almasirad[3,*], and Mona Salimi[2,*]

[1]Department of Biology, Faculty of Science, University of Guilan, Rasht, I.R. Iran.
[2]Department of Physiology and Pharmacology, Pasteur Institute of Iran, Tehran, I.R.Iran.
[3]Department of Medicinal Chemistry, Faculty of Pharmacy, Tehran Medical Sciences, Islamic Azad University, Tehran, I.R. Iran.

Abstract

Background and purpose: Considering various studies implying anticancer activity of the hydrazone and oxamide derivatives through different mechanisms such as kinases and calpain inhibition, herein, we report the synthesis, characterization, and evaluation of the antiproliferative effect of a series of hydrazones bearing oxamide moiety compounds (**7a-7n**) against a panel of cancer cell lines to explore a novel and promising anticancer agent (**7k**).
Experimental approach: Chemical structures of the synthesized compounds were confirmed by FTIR, ^{1}H-NMR, ^{13}C-NMR, and mass spectra. The antiproliferative activity and cell cycle progression of the target compound were investigated using the MTT assay and flow cytometry.
Findings/Results: Compound **7k** with 2-hydroxybenzylidene structure was found to have a significant *in vitro* anti-proliferative influence on MDA-MB-231 (human adenocarcinoma breast cancer) and 4T1 (mouse mammary tumor) cells as the model of triple-negative breast cancer, with the $IC_{50\text{-}72\ h}$ values of 7.73 ± 1.05 and 1.82 ± 1.14 µM, respectively. Following 72-h incubation with compound **7k**, it caused MDA-MB-231 cell death through G1/S cell cycle arrest at high concentrations (12 and 16 µM).
Conclusion and implications: Conclusively, this study for the first time reports the anti-proliferative efficacy of compound **7k** possessing 2-hydroxyphenyl moiety, which may serve as a potent candidate in triple-negative breast cancer treatment.

Keywords: Anti-proliferation; Cancer; Cell Cycle; Hydrazone; Oxamide.

INTRODUCTION

Since the beginning of the twenty-first century, cancer has been a major leading cause of death globally with a significant economic burden in all countries (1). Breast cancer as one of the most common cancers in women has become a major concern threatening women's health with an annually increasing number of patients (2). Among all breast cancers, triple-negative breast cancer (TNBC) has a metastatic pattern with a poor prognosis (3). In other words, it is of particular research interest as triple-negative breast cancer is therapeutically challenging mainly due to its low response to chemotherapeutics and highly aggressive features (4). Despite the significant progress made in research and the development of breast cancer drugs, drug resistance has remained one of the major clinical obstacles needed to be resolved (5). Thus, developing novel compounds to fight this fatal disease remains urgent and of great importance.

*Corresponding authors:
A. Almasirad, Tel: +98-2122640051, Fax: +98-22602059
Email: almasirad.a@iaups.ac.ir
M. Salimi, Tel: +98-2164112264, Fax: +98-2164112834
Email: salimimona@pasteur.ac.ir

Access this article online

Website: http://rps.mui.ac.ir

DOI: 10.4103/1735-5362.363593

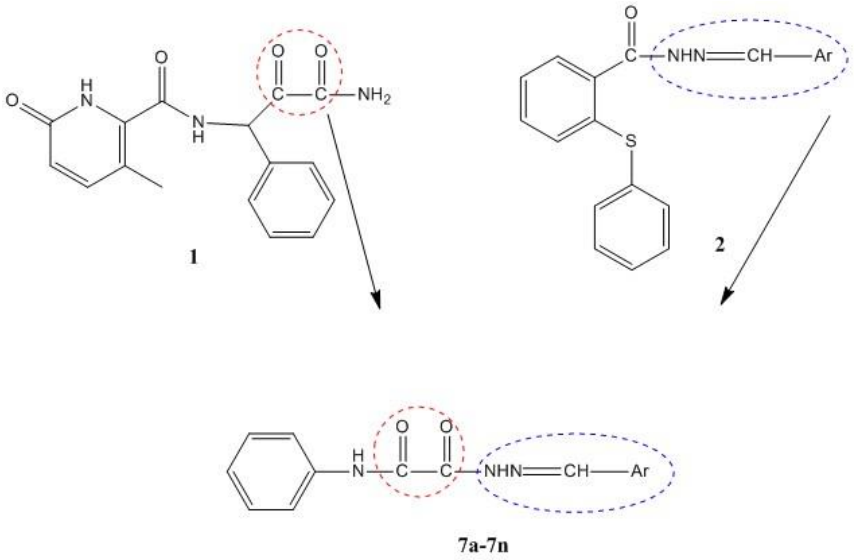

Scheme 1. Design of target compounds.

In the strategy of drug design, connecting various pharmacophores with similar activity and subsequently preparing the hybrid molecules results in the development of novel drugs. In this context, the hydrazone group as a promising pharmacophore presents richly in medicinal molecules and contributes a significant role to discover a wide range of therapeutic agents with several biological and chemotherapeutic activities (6-9). Among the various bioactivities reported for hydrazone derivatives including anti-malarial, anti-tuberculosis, and anti-HIV, our attention has been drawn toward their anticancer properties (9). Besides, oxamide compounds exert their anticancer effects through different mechanisms such as inhibition of calpain, histone deacetylase, protein-tyrosine phosphatase, tyrosine kinase, beta-tubulin inhibition, cyclin-dependent kinase 4 inhibition, upregulation of integrin beta 4, induction of apoptosis (10-19). Moreover, the short half-life and low oral bioavailability of the oxamides caused that several compounds possessing this pharmacophore have been noticed (20). Altogether, oxamide and hydrazone groups are found in a great number of anticancer agents such as compounds **1** and **2** in Scheme 1 (9,21-22).

Based on the aforementioned findings, herein, a series of hybrid compounds in which hydrazone and oxamide pharmacophores were covalently associated into a single molecule (**7a-7n**), were synthesized and assessed for their potential antiproliferative activity. Indeed, the target structures bearing together oxamide and hydrazone moieties may act as dual anticancer functional groups.

MATERIALS AND METHODS

General

Chemicals used in the chemistry experiment were purchased from Merck and Sigma/Aldrich Companies. Melting points were taken on an electrothermal IA 9300 capillary melting-point apparatus (Ontario, Canada) and are uncorrected. Proton and carbon-13 nuclear magnetic resonance (^{1}H-NMR and ^{13}C-NMR) spectra were obtained using Bruker FT-250 or FT-500 spectrometers (Bruker, Rheinstetten, Germany). Mass spectra were obtained using a 5973 Network Mass Selective Detector at 70 eV (Agilent technology, USA). Fourier-transform infrared spectroscopy (FTIR) spectra were recorded by Shimadzu FT-IR 8400S spectrographs (KBr disks, Japan). Elemental analysis was carried out using a Perkin-Elmer Model 240-c apparatus (Perkin Elmer, Norwalk, CT, USA). The results of the elemental analyses (C, H, N) were within ± 0.4% of the calculated amount.

Human breast cancer cell lines, MDA-MB-231 (C578) and MCF-7 (C135), human colorectal adenocarcinoma cell line HT-29 (C466), hepatocarcinoma cell line Hep-G2

(C158), and normal human skin fibroblast cell line HSF (C192) were provided from the National Cell Bank of Pasture Institute of Iran (NCBI). Dulbecco's modified eagle's medium (DMEM), FBS (fetal bovine serum), trypsin-ethylenediaminetetraacetic acid (EDTA), and penicillin G/streptomycin were purchased from Gibco (Gibco-BRL, Rockville, IN, USA). The 3−(4,5−dimethylthiazol−2−yl) 2,5−diphenyl-tetrazolium (MTT) was obtained from Sigma-Aldrich (Saint Louis, Missouri, USA). The other chemicals were supplied by Merck (Darmstadt, Germany) and Sigma-Aldrich (St Louis, MO, USA).

Chemistry

The fourteen designed compounds were synthesized starting with a reaction of aniline **3** with ethyl oxalyl chloride **4** to give intermediate **5** (22). Hydrazide **6** was prepared by the treatment of **5** with hydrazine hydrate (23). Final compounds (**7a-7n)** were synthesized through acid-catalyzed condensation of **6** with the corresponding aldehydes (Scheme 2). Synthesis of compounds **7a, 7h, 7i, 7j,** and **7k** has been reported previously; however, ten compounds are novel and reported here for the first time (23-29).

Synthesis of ethyl oxo(phenylamino)acetate (5)

To a stirring solution of aniline **3** (1.8 mL, 20 mmol) and triethylamine (2.8 mL, 20 mmol) in dichloromethane (60 mL) at 0 °C, a solution of ethyl oxalyl chloride **4** (2.2 mL, 20 mmol) in 20 mL dichloromethane was slowly added and then the reaction was stirred for 1 h in this condition. The mixture was stirred at room temperature for another 1 h and the solvent was evaporated to give 3.74 g of compound **5** with a yield of 98% and the melting point of 66-67 °C used in the next step without further purification. IR (KBr): νcm^{-1} 3346 (NH, stretch), 1704 (C=O, stretch) (26).

Synthesis of 2-hydrazinyl-2-oxo-N-phenyl-acetamide (6)

To a solution of (3.74 g, 19 mmol) compound **5** in 96% ethanol, 135 mL of hydrazine hydrate (1.13 mL, 23 mmol) was added dropwise. The resulting solution was stirred at room temperature for 2 h and the precipitate was filtered off to give 3.12 g of compound **6** with a yield of 90% and a melting point of 217-219 °C (26), which was used in the next step without further purification. IR (KBr): νcm^{-1} 3319, 3284 (NH2, NH, stretch), 1668 (C=O, stretch).

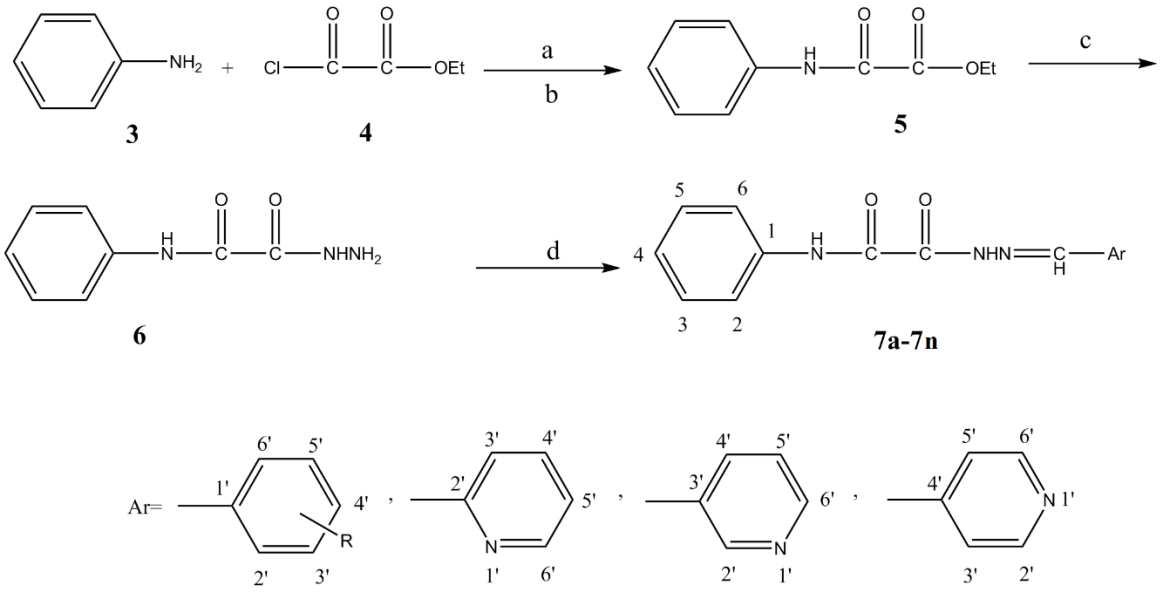

7a= Phenyl, 7b= 2-Chlorophenyl, 7c= 3-chlorophenyl, 7d= 4-chlorophenyl, 7e= 2-Bromophenyl, 7f= 3-Bromophenyl, 7g= 4-bromophenyl, 7h=2-Nitrophenyl, 7i= 3-Nitrophenyl, 7j= 4-Nitrophenyl, 7k= 2-Hydroxyphenyl, 7l= 2-pyridyl, 7m= 3-pyridyl, 7n= 4-pyridyl

Scheme 2. Reagent and conditions: (a) triethylamine, CH_2Cl_2, stir, 0 °C, 1 h; (b) stir, room temperature, 1 h; (c) hydrazine hydrate, EtOH, stir, room temperature, 2 h; (d) Ar-CHO, EtOH, HCl, stir, room temperature, 2 h.

General procedure for the preparation of compounds 7a-7n

A solution of **6** (3.55 mmol), corresponding aldehydes (3.57 mmol), and HCl 37% (2 drops) in 96% ethanol (40 mL) were stirred for 2 h at room temperature. To the resulting mixture, $NaHCO_3$ (10%) was added and the precipitate was filtered off and washed with water, and recrystallized from the suitable solvent.

Cell growth inhibition assay

Synthesized compounds (**7a-7n**) were dissolved in dimethyl sulfoxide (DMSO, 0.5%), and cells were then treated with the appropriate concentrations (1-50 µM) of the compounds. Untreated cells, 0.5% DMSO- and doxorubicin-treated cells served as the negative, vehicle, and positive control cells, respectively. Viability is defined as the ability of chemical compounds to transform MTT into purple-blue formazan salt. Indeed, the amount of visible formazan crystals in each well is directly proportional to the number of living cells (30). The number of 1-5 × 10^3 cells/well for MDA-MB-231, 3-7 × 10^3 cells/well for MCF7, 3-7 × 10^3cells/well for HT-29, 4-8 × 10^3 cells/well for Hep-G2, and 0.5-3.5 × 10^3 cells/well for 4T1 were cultured in 96-well plates and kept to be attached overnight. In the initial screening, the antiproliferative activity of the compounds was calculated at a unique concentration (50 µM) at 72 h and then the half maximal inhibitory concentration (IC_{50}) values were measured for the selected compound at 24, 48, and 72 h towards MDA-MB-231 cells. Moreover, the number of 2 × 10^3 cells of HSF was seeded to measure the viability on a normal cell line. To determine cell growth inhibition in each well, 20 µL of MTT solution (5 mg/mL in PBS) was added and incubated at 37 °C for 4 h. Following the formation of the visible formazan crystals by mitochondrial succinate dehydrogenase in the live cells, they were solubilized in DMSO and the optical density was measured at 570 nm using an ELISA plate reader (Epoch2, Biotek, USA). Relative cell growth inhibition was calculated compared to the non-treated cells.

Analysis of cell cycle progression

The impact of compound **7k** on cell cycle progression was assessed using propidium iodide (PI) staining. MDA-MB-231 and 4T1 cells with a density of about 3 × 10^4 and 2.5 × 10^4 cells/well were subjected to compound **7k** at 8, 12, 16 µM, and 2, 4, 8 µM concentrations, respectively, for 72 h. After trypsinization, the cells were fixed using 70% ethanol for 24 h at -20 °C. Then, the samples were stained whit PI (1 mg/mL), Triton^{TM} X-100 (0.1%), and RNAse (100 mg/mL) and incubated for 15 min in a dark place at 37 °C. The percentage of cell populations in the G0/G1, S, and G2/M phases of the cell cycle was determined with the PARTEC flow cytometer (PARTEC GmbH, Munster, Germany) using FlowJo software. Cell cycle phases were determined by recording the peak area of FL3-A on a linear scale. Samples were prepared in triplicates with at least three repetitions for each experiment (9).

Statistical analysis

Experimental data were analyzed statistically using Graph Pad Prism 6 Software (GraphPad Software, La Jolla, CA, United States). The values are expressed as mean ± SEM of at least triplicates. Data were assessed using one-way ANOVA followed by Tukey's multiple comparison test. *P*-values < 0.05 were considered statistically significant.

RESULTS

Chemistry

A diverse array of derivatives (**7a-7n**) was synthesized and then characterized by physical and spectral data (FTIR, ^{1}H-NMR, ^{13}C-NMR, Mass) (Fig. 1).

*2-[2-Benzylidenehydrazinyl]-2-oxo-N-phenyl-acetamide (**7a**)*

Melting point (m.p) = 274-276 °C (EtOH) (25), yield 85%, IR (KBr): ν cm^{-1} 3292, 3249 (NH, stretch), 1656 (C=O, stretch). ^{1}H-NMR (250 MHz, DMSO-d_6): δppm 12.33 (s, 1H, NH), 10.81 (s, 1H, NH), 8.62 (s, 1H, N=CH), 7.86 (d, *J*=7.7 Hz, 2H, H_2, H_6), 7.73-7.71 (m, 2H, $H_{2'}$, $H_{6'}$), 7.47-7.44 (m, 3H, $H_{3'}$, $H_{4'}$, $H_{5'}$), 7.37 (t, *J* = 7.7 Hz, 2H, H_3, H_5), 7.15 (t, *J* = 7.2, 1H, H_4).^{13}C-NMR (60 MHz, DMSO-d_6): δppm 158.77 (C=O), 157.01 (C=O), 151.56 (=C), 137.99 (C-1), 134.29 (C-1'), 131.06 (C-4'), 129.34 (C-2', C-6'), 129.17 (C-3, C-5), 127.88 (C-3', C-5'), 125.10 (C-4), 120.99 (C-2, C-6). Mass: m/z (%) 267 (M^+, 33), 147 (100), 119 (39), 120 (26), 92 (24), 93 (28), 77 (44), 51 (15). Anal. Calcd. for $C_{15}H_{13}N_3O_2$: C, 67.40; H, 4.90; N, 15.72. Found: C, 67.19; H, 4.83; N, 15.53.

A1

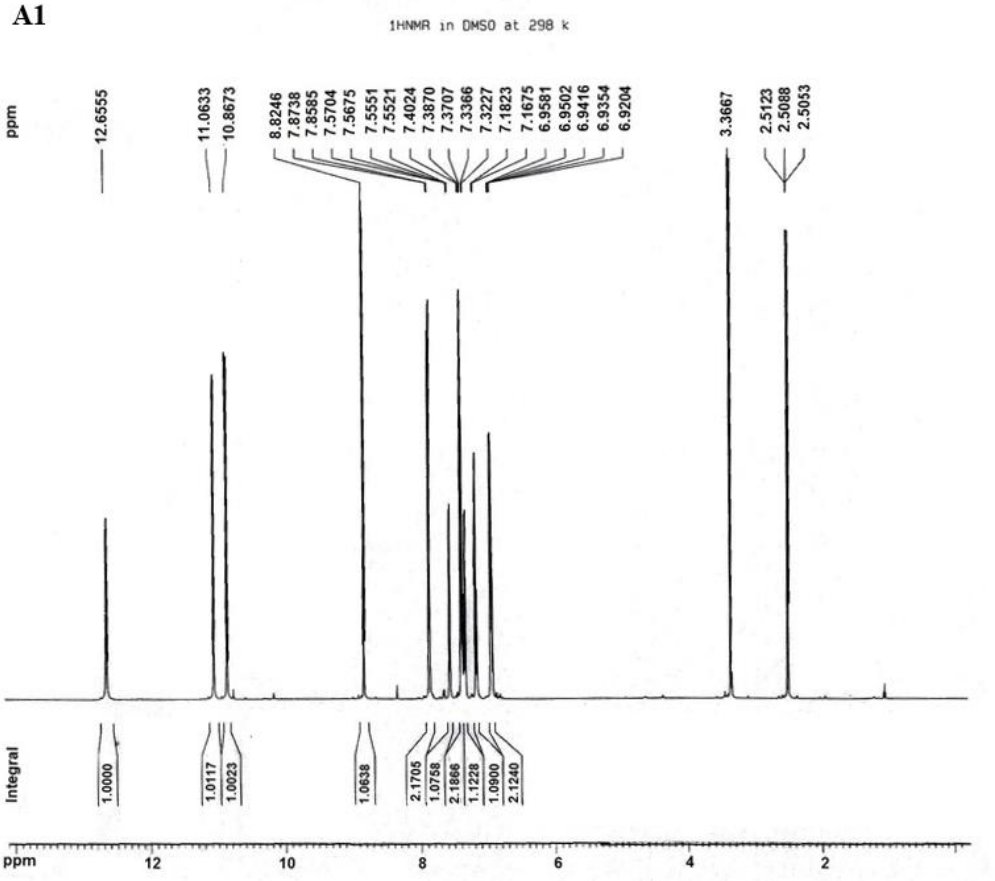
1HNMR in DMSO at 298 k
ppm
12.6555
11.0633
10.8673
8.8246
7.8738
7.8585
7.5704
7.5675
7.5551
7.5521
7.4024
7.3870
7.3707
7.3366
7.3227
7.1823
7.1675
6.9581
6.9502
6.9416
6.9354
6.9204
3.3667
2.5123
2.5088
2.5053
Integral
1.0000
1.0117
1.0023
1.0638
2.1705
1.0758
2.1866
1.1228
1.0900
2.1240
ppm
12
10
8
6
4
2

A2

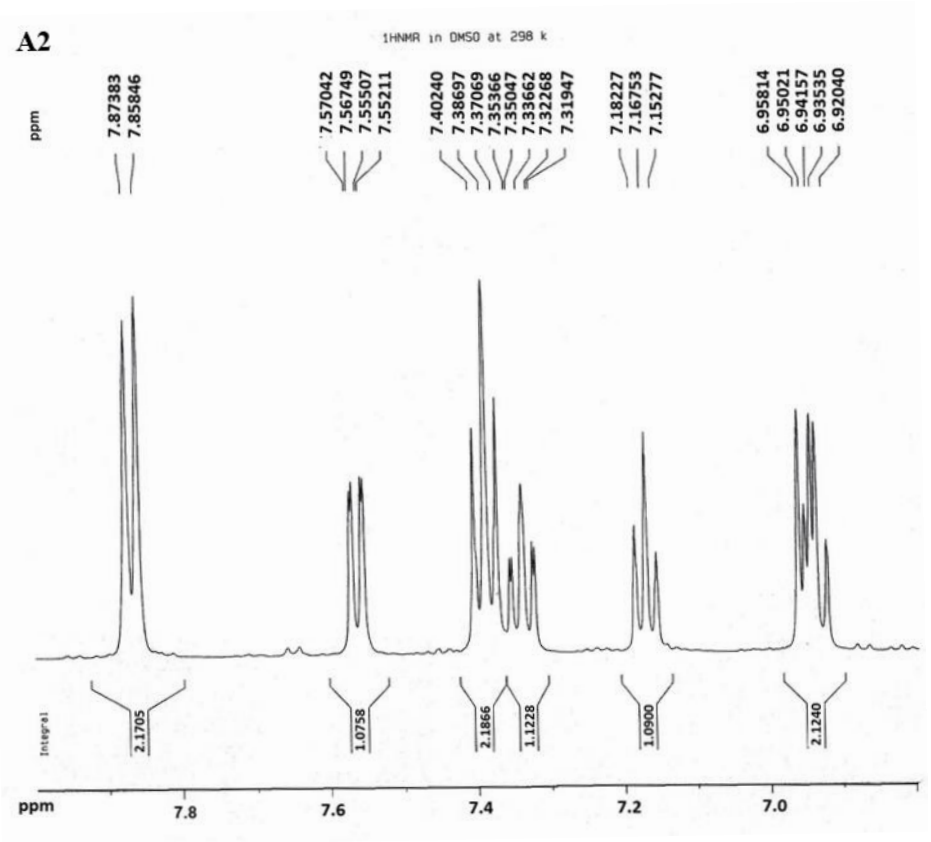
1HNMR in DMSO at 298 k
ppm
7.87383
7.85846
7.57042
7.56749
7.55507
7.55211
7.40240
7.38697
7.37069
7.35366
7.35047
7.33662
7.32268
7.31947
7.18227
7.16753
7.15277
6.95814
6.95021
6.94157
6.93535
6.92040
Integral
2.1705
1.0758
2.1866
1.1228
1.0900
2.1240
ppm
7.8
7.6
7.4
7.2
7.0

B1

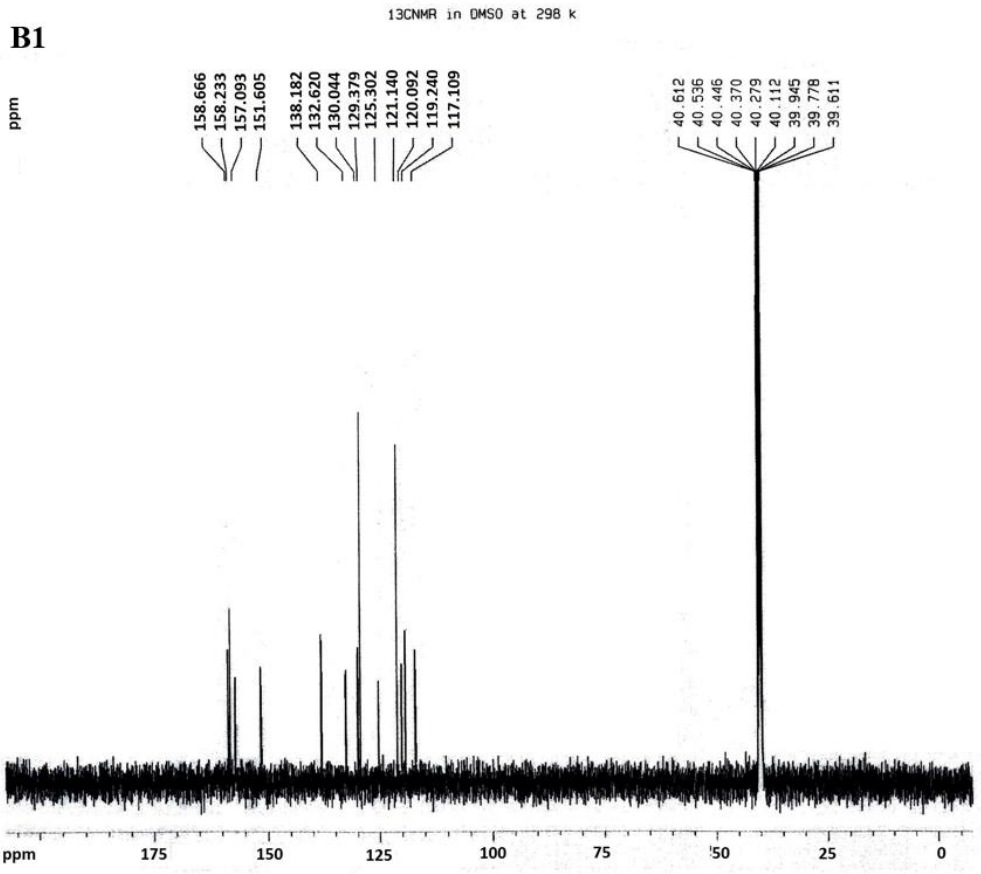
13CNMR in DMSO at 298 k
ppm
158.666
158.233
157.093
151.605
138.182
132.620
130.044
129.379
125.302
121.140
120.092
119.240
117.109
40.612
40.536
40.446
40.370
40.279
40.112
39.945
39.778
39.611
ppm
175
150
125
100
75
50
25
0

B2

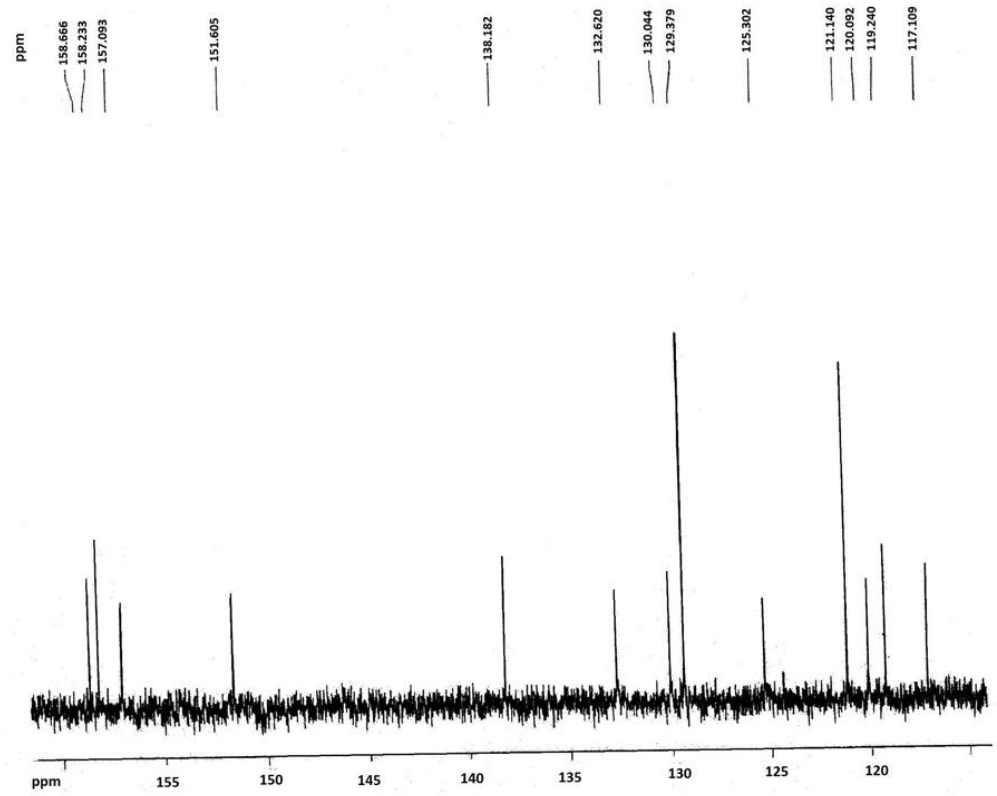
ppm
158.666
158.233
157.093
151.605
138.182
132.620
130.044
129.379
125.302
121.140
120.092
119.240
117.109
ppm
155
150
145
140
135
130
125
120

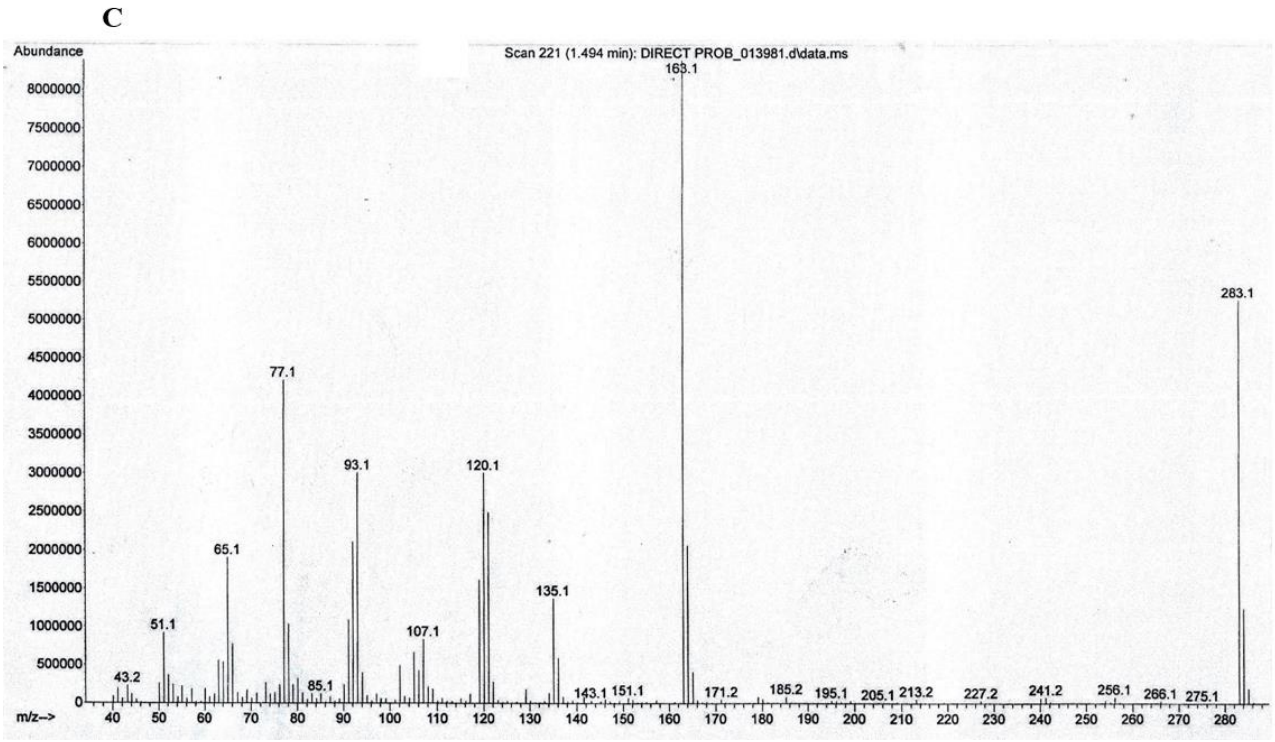

Fig. 1. Spectral data (A1 and A2) ^{1}H-NMR (B1 and B2) ^{13}C-NMR and (C) mass of compound **7k** as the most potent antiproliferative compound.

*2-[2-(2-Chlorobenzylidene)hydrazinyl]-2-oxo-N-phenylacetamide **(7b)***

m.p = 240-241 °C (EtOH), yield 95%, IR (KBr): νcm^{-1} 3292, 3251 (NH, stretch), 1662 (C=O, stretch). ^{1}H-NMR (250 MHz, DMSO-d_6): δppm 12.54 (s, 1H, NH), 10.74 (s, 1H, NH), 8.98 (s, 1H, N=CH), 7.94 (d, *J* = 7.0 Hz, 1H, H_6'), 7.77 (d, *J* = 7.8 Hz, 2H, H_2, H_6), 7.47-7.26 (m, 5H, H_3, H_5, H_3', H_4', H_5'), 7.07 (t, *J* = 7.3 Hz, 1H, H_4). ^{13}C-NMR (60 MHz, DMSO-d_6): δppm 158.6 (C=O), 157.2 (C=O), 147.6 (=C), 137.9 (C-1), 134.1 (C-2'), 132.4 (C-1'), 131.7 (C-4'), 130.4 (C-6'), 129.2 (C-3 and C-5), 128.1 (C-3'), 127.6 (C-5'), 125.1 (C-4), 120.9 (C-2 and C-6). Mass: m/z (%) 303 (M^++2, 6), 301 (M+, 17), 181 (100), 164 (37), 119 (45), 93 (33), 77 (55), 51 (15). Anal. Calcd. for $C_{15}H_{12}ClN_3O_2$: C, 59.71; H, 4.01; N, 13.93. Found: C, 60.02; H, 4.11; N, 13.84.

*2-[2-(3-Chlorobenzylidene) hydrazinyl]-2-oxo-N-phenylacetamide **(7c)***

m.p = 243-245 °C (EtOH), yield 94%, IR (KBr): νcm^{-1} 3303, 3255 (NH, stretch), 1660 (C=O, stretch). ^{1}H-NMR (250 MHz, DMSO-d_6): δppm 12.54 (s, 1H, NH), 10.91 (s, 1H, NH), 8.64 (s, 1H, N=CH), 7.91 (d, *J* = 8.3 Hz, 2H, H_2, H_6), 7.81 (s, 1H, H_2'), 7.72 (d, 1H, *J* = 6.0 Hz, 1H, H_6'), 7.57-7.51 (m, 2H, H_4', H_5'), 7.42 (t, *J* = 8.0 Hz, 2H, H_3, H_5), 7.20 (t, *J* = 7.0 Hz, 1H, H_4). ^{13}C-NMR (60 MHz, DMSO-d_6): δppm 158.6 (C=O), 157.2 (C=O), 149.8 (=C), 138.0 (C-1), 136.5 (C-1'), 134.1 (C-3'), 131.3 (C-4'), 130.7 (C-2'), 129.2 (C-3 and C-5), 126.9 (C-6'), 126.7 (C-5'), 125.1 (C-4), 120.9 (C-2 and C-6). Mass: m/z (%) 303 (M^++2, 5), 301 (M+, 15), 293 (33), 181 (100), 119 (41), 77 (47), 51 (12). Anal. Calcd. for $C_{15}H_{12}ClN_3O_2$: C, 59.71; H, 4.01; N, 13.93. Found: C, 59.98; H, 4.18; N, 13.81.

*2-[2-(4-Chlorobenzylidene)hydrazinyl]-2-oxo-N-phenylacetamide **(7d)***

m.p = 299-300 °C (EtOAc), yield 93%, IR (KBr): νcm^{-1} 3301, 3256 (NH, stretch), 1697, 1662 (C=O, stretch). ^{1}H-NMR (250 MHz, DMSO-d_6): δppm 12.32 (s, 1H, NH), 10.74 (s, 1H, NH), 8.52 (s, 1H, N=CH), 7.76 (d, *J* = 7.7 Hz, 2H, H_2, H_6), 7.66 (d, *J* = 8.5 Hz, 2H, H_2', H_6'), 7.45 (d, *J* = 8.5 Hz, 2H, H_3', H_5'), 7.29 (t, *J* = 7.7 Hz, 2H, H_3, H_5), 7.07 (t, *J* = 7.3 Hz, 1H, H_4). ^{13}C-NMR (60 MHz, DMSO-d_6): δppm 158.7 (C=O), 157.0 (C=O), 150.1 (=C), 138.0 (C-1), 135.5 (C-4'), 133.2 (C-1'), 129.5 (C-2', C-3', C-5', C-6'), 129.2 (C-3 and C-5), 125.1 (C-4), 121.0 (C-2 and C-6). Mass: m/z (%) 303 (M^+ +

2, 11), 301 (M+, 33), 181 (100), 153 (21), 120 (31), 93 (33), 77 (58), 51 (15). Anal. Calcd. for $C_{15}H_{12}ClN_3O_2$: C, 59.71; H, 4.01; N, 13.93. Found: C, 59.59.55; H, 9.97; N, 13.13.79.

2-[2-(2-Bromobenzylidene)hydrazinyl]-2-oxo-N-phenylacetamide ***(7e)***

m.p = 237-240 °C (EtOH), yield 86%, IR (KBr): νcm^{-1} 3286, 3247 (NH, stretch), 1660 (C=O, stretch).^{1}H-NMR (250 MHz, DMSO-d_6): δppm 12.65 (s, 1H, NH), 10.81 (s, 1H, NH), 9.02 (s, 1H, N=CH), 7.99 (d, *J* = 7.5 Hz, 1H, H_3'), 7.85 (d, *J* = 8.0 Hz, 2H, H_2, H_6), 7.70 (d, *J* = 7.7 Hz, 1H, H_6'), 7.50-7.33 (m, 4H, H_3, H_5, H_4', H_5'), 7.15 (t, *J* = 7.2 Hz, 1H, H_4) . ^{13}C-NMR (60 MHz, DMSO-d_6): δppm 158.61 (C=O), 157.26 (C=O), 149.97 (=C), 137.99 (C-1), 133.68 (C-1'), 133.26 (C-4'), 132.67 (C-3'), 129.17 (C-3, C-5), 128.57 (C-6'), 127.99 (C-5'), 125.11 (C-2'), 124.40 (C-4'), 120.98 (C-2, C-6). Mass: m/z (%) 347 (M^++2, 3), 345 (M+, 3), 227 (39), 225 (39), 119 (28), 92 (30), 77 (100), 65 (26), 51 (14). Anal. Calcd. for $C_{15}H_{12}BrN_3O_2$: C, 52.04; H, 3.49; N, 12.14. Found: C, 52.37; H, 3.38; N, 12.40.

2-[2-(3-Bromobenzylidene)hydrazinyl]-2-oxo-N-phenylacetamide ***(7f)***

m.p = 235-237 °C (MeCN), yield 83%, IR (KBr): νcm^{-1} 3268, 3242 (NH, stretch), 1662 (C=O, stretch). ^{1}H-NMR (250 MHz, DMSO-d_6): δppm 12.49 (s, 1H, NH), 10.85 (s, 1H, NH), 8.57 (s, 1H, N=CH), 7.9 (s, 1H, H_2'), 7.85 (d, *J* = 8 Hz, 2H, H_2, H_6), 7.72-7.63 (m, 2H, H_4', H_6'), 7.46-7.34 (m, 3H, H_3, H_5, H_5'), 7.15 (t, *J* = 7.0 Hz, 1H, H_4). ^{13}C-NMR (60 MHz, DMSO-d_6): δppm 158.62 (C=O), 157.15 (C=O), 149.76 (=C), 137.97 (C-1'), 136.69 (C-1), 133.59 (C-4'), 131.56 (C-2'), 129.79 (C-5'), 129.18 (C-3, C-5), 127.08 (C-6'), 125.13 (C-3'), 122.65 (C-4), 120.98 (C-2, C-6). Mass: m/z (%) 347 (M^++2, 7), 345 (M^+, 7), 227 (42), 225 (42), 120 (19), 92 (30), 77 (100), 65 (25), 51 (14). Anal. Calcd. for $C_{15}H_{12}BrN_3O_2$: C, 52.04; H, 3.49; N, 12.14. Found: C, 52.15; H, 3.62; N, 12.45.

2-[2-(4-Bromobenzylidene)hydrazinyl]-2-oxo-N-phenylacetamide ***(7g)***

m.p = 311-315 °C (THF), yield 87%, IR (KBr): νcm^{-1} 3299, 3245 (NH, stretch), 1664 (C=O, stretch). ^{1}H-NMR (250 MHz, DMSO-d_6): δppm 12.39 (s, 1H, NH), 10.81 (s, 1H, NH), 8.59 (s, 1H, N=CH), 7.85 (d, *J* = 7.7 Hz, 2H, H_2, H_6), 7.65 (bs, 4H, H_2', H_3', H_5', H_6'), 7.35 (t, *J* = 7.7 Hz, 2H, H_3, H_5), 7.14 (t, *J* = 7.2 Hz, 1H, H_4). ^{13}C-NMR (60 MHz, DMSO-d_6): δppm 158.67 (C=O), 157.05 (C=O), 150.31 (=C), 137.97 (C-1), 133.55 (C-1'), 132.35 (C-3', C-5'), 129.69 (C-2', C-6'), 129.15 (C-3, C-5), 125.10 (C-4'), 124.37 (C-4), 120.99 (C-2, C-6). Mass: m/z (%) 347 (M^++2, 12), 345 (M+, 12), 227 (41), 225 (41), 118 (22), 92 (30), 77 (100), 65 (26), 51 (13). Anal. Calcd. for C15H12BrN3O2: C, 52.04; H, 3.49; N, 12.14. Found: C, 51.85; H, 3.34; N, 12.30.

2-[2-(2-Nitrobenzylidene)hydrazinyl]-2-oxo-N-phenylacetamide ***(7h)***

m.p = 260-262 °C (EtOAc) (26), yield 96%, IR (KBr): νcm^{-1} 3294, 3255 (NH, stretch), 1699 (C=O, stretch), 1662 (C=O, stretch), 1523, 1348 (NO_2). ^{1}H-NMR (250 MHz, DMSO-d_6): δppm 12.63 (s, 1H, NH), 10.75 (s, 1H, NH), 8.94 (s, 1H, N=CH), 8.03-7.99 (m, 2H, H_3', H_6'), 7.75 (d, *J* = 7.7 Hz, 3H, H_2, H_6, H_5'), 7.66-7.60 (m, 1H, H_4'), 7.29 (t, *J* = 7.8 Hz, 2H, H_3, H_5), 7.07 (t, *J* = 7.3 Hz, 1H, H_4). ^{13}C-NMR (60 MHz, DMSO-d_6): δppm 158.5 (C=O), 157.5 (C=O), 148.8 (C-2'), 147.0 (=C), 137.9 (C-1), 134.3 (C-5'), 131.6 (C-4'), 129.2 (C-3 and C-5), 128.8 (C-1' and C-6'), 125.1 (C-4), 121.0 (C-2 and C-6 and C-3'). Mass: m/z (%) 312 (M^+, 13), 192 (100), 164 (40), 120 (66), 92 (59), 77 (80), 51 (24). Anal. Calcd. for $C_{15}H_{12}N_4O_4$: C, 57.69; H, 3.87; N, 17.94. Found: C, 57.38; H, 3.99; N, 17.68.

2-[2-(3-Nitrobenzylidene)hydrazinyl]-2-oxo-N-phenylacetamide ***(7i)***

m.p = 260-264 °C (THF) (25), yield 80%, IR (KBr): νcm^{-1} 3286, 3234 (NH, stretch), 1664 (C=O, stretch), 1520, 1353 (NO_2, stretch). ^{1}H-NMR (500 MHz, DMSO-d_6) : δppm 12.62 (s, 1H, NH), 8.74 (s, 1H, N=CH), 8.53 (s, 1H, H_2'), 8.31 (dd, *J* = 8.2, 1.3 Hz, 1H, H_4'), 8.15 (d, *J* = 7.7 Hz, 1H, H_6'), 7.87 (d, *J* = 7.9 Hz, 2H, H_2, H_6), 7.78 (t, *J* = 8 Hz, 1H, H_5'), 7.39 (t, *J* = 7.9 Hz, 2H, H_3, H_5), 7.17 (t, *J* = 7.5 Hz, 1H, H_4). ^{13}C-NMR (125 MHz, DMSO-d_6): δppm 158.77(C=O), 157.47(C=O), 149.34(C-3'), 148.85 (C=N), 138.16 (C-1), 136.25 (C-6'), 134.34 (C-1'), 131.24 (C-5'), 129.37 (C-3, C-5),

125.44, 125.33, 121.88, 121.19. Mass: m/z (%) 312 (M^+, 30), 192 (100), 120 (37), 92 (52), 77 (94), 65 (33), 51 (22). Anal. Calcd. $C_{15}H_{12}N_4O_4$: C, 57.69; H, 3.87; N, 17.94. Found: C, 57.87; H, 3.80; N, 17.18.17.

2-[2-(4-Nitrobenzylidene)hydrazinyl]-2-oxo-N-phenylacetamide ***(7j)***

m.p = 317-320 °C (EtOH) (25), yield 86%, IR (KBr): νcm^{-1} 3302, 3256 (NH, stretch), 1660 (C=O, stretch), 1525, 1346 (NO_2, stretch). ^{1}H-NMR (500 MHz, DMSO-d_6): δppm 12.65 (s, 1H, NH), 10.89 (s, 1H, NH), 8.72 (s, 1H, N=CH), 8.31 (d, *J* = 8.7 Hz, 2H, H_3', H_5'), 7.98 (d, *J* = 8.7 Hz, 2H, H_2', H_6'), 7.87 (d, 2H, *J* = 7.9 Hz, H_2, H_6), 7.39 (t, *J* =7.9 Hz, 2H, H_3, H_5), 7.17 (t, *J* = 7 Hz, 1H, H_4). ^{13}C-NMR (125 MHz, DMSO-d_6): δppm 158.69 (C=O), 157.53 (C=O), 149.21 (C4'), 148.80 (=C), 140.65 (C-1'), 138.15 (C-1), 129.37 (C-2', C-6'), 129.03 (C-3, C-5), 125.34 (C-4), 124.75 (C-3', C-5'), 121.19 (C-2, C-6). Mass: m/z (%) 312 (M^+, 33), 192 (100), 120 (30), 92 (30), 77 (41), 65 (12), 51 (7). Anal. Calcd. for $C_{15}H_{12}N_4O_4$: C, 57.69; H, 3.87; N, 17.94. Found: C, 57.81; H, 3.65; N, 17.81.

2-[2-(2-Hydroxybenzylidene)hydrazinyl]-2-oxo-N-phenylacetamide ***(7k)***

m.p = 253-266 °C (EtOH) (24), yield 90%, IR (KBr): νcm^{-1} 3339 (OH, stretch), 3303, 3260 (NH, stretch), 1663 (C=O, stretch). ^{1}H-NMR (500 MHz, DMSO-d_6): δppm 12.65 (s, 1H, NH), 11.06 (s, 1H, OH), 10.87 (s, 1H, NH), 8.82 (s, 1H, N=CH), 7.86 (d, *J* = 7.7 Hz, 2H, H_2, H_6), 7.56 (dd, *J* = 7.7, 1.5, Hz, 1H, H_6'), 7.39 (t, *J* = 7.7 Hz, 2H, H_3, H_5), 7.35-7.31 (m, 1H, H_4'), 7.17 (t, *J* = 7.5 Hz, 1H, H_4), 6.95-6.92 (m, 2H, H_3', H_5'). ^{13}C-NMR (125 MHz, DMSO-d_6): δppm 158.67 (C=O), 158.23 (C-2'), 157.09 (C=O), 151.61 (=C), 138.18 (C-1), 132.62 (C-4'), 130.04 (C-6'), 129.38 (C-3, C-5), 125.30 (C-4), 121.14 (C-2, C-6), 120.09 (C-6'), 119.24 (C-1'), 117.11 (C-3'). Mass: m/z (%) 283 (M^+, 63), 163 (100), 135(16), 120 (36), 93 (36), 77 (41), 65 (12), 51 (7). Anal. Calcd. $C_{15}H_{13}N_3O_3$: C, 63.60; H, 4.63; N, 14.83. Found: C, 63.88; H, 4.75; N, 14.64.

2-[2-(Pyridin-2ylmethylidene)hydrazinyl]-2-oxo-N-phenylacetamide ***(7l)***

m.p = 248-250 °C (EtOH), yield 94%, IR (KBr): νcm^{-1} 3290 (NH, stretch), 1670 (C=O, stretch). ^{1}H-NMR (250 MHz, DMSO-d_6): δppm 12.72 (s, 1H, NH), 10.94 (s, 1H, NH), 8.73 (s, 1H, N=CH), 8.67 (d, *J* = 4.7 Hz, 1H, H_6'), 8.04 (d, *J* = 7.7 Hz, 1H, H_3'), 7.93 (d, *J* = 7.7 Hz, 2H, H_2, H_6), 7.89-7.85 (m, 1H, H_4'), 7.50-7.39 (m, 3H, H_3, H_5, H_5'), 7.19 (t, *J* = 7.3 Hz, 1H, H_4). ^{13}C-NMR (60 MHz, DMSO-d_6): δppm 158.5 (C=O), 157.3 (C=O), 153.3 (C-2'), 151.7 (C-6'), 150.0 (=C), 137.9 (C-4'), 137.3 (C-1), 129.2 (C-3 and C-5), 125.2 (C-4), 125.1 (C-5'), 121.0 (C-2 and C-6), 120.1 (C-3'). Mass: m/z (%) 268 (M^+, 6), 179 (4), 148 (100), 120 (74), 92 (96), 77 (52), 65 (59), 51 (30). Anal. Calcd. for $C_{14}H_{12}N_4O_2$: C, 62.68; H, 4.51; N, 20.88. Found: C, 62.39; H, 4.14; N, 20.73.

2-[2-(Pyridin-3ylmethylidene)hydrazinyl]-2-oxo-N-phenylacetamide ***(7m)***

m.p = 255-256 °C (EtOH), yield 92%, IR (KBr): νcm^{-1} 3296, 3244 (NH, stretch), 1664 (C=O, stretch). ^{1}H-NMR (250 MHz, DMSO-d_6): δppm 12.59 (s, 1H, NH), 10.91 (s, 1H, NH), 8.89 (s, 1H, H_2'), 8.72 (s, 1H, N=CH), 8.67 (d, *J* = 4.5 Hz, 1H, H_6'), 8.18 (d, *J* = 6.5, 1H, H_4'), 7.92 (d, *J* = 8.0 Hz, 2H, H_2, H_6), 7.54 –7.49 (m, 1H, H_5'), 7.41 (t, *J* = 8.0 Hz, 2H, H_3, H_5), 7.19 (t, *J* = 7.0 Hz, 1H, H_4). ^{13}C-NMR (60MHz, DMSO-d_6): δppm 158.6 (C=O), 157.1 (C=O), 151.6 (C-6'), 149.4 (C-2'), 148.8 (=C), 138.0 (C-1), 134.3 (C-4'), 130.2 (C-3'), 129.2 (C-3 and C-5), 125.1 (C-5'), 124.5 (C-4), 121.0 (C-2 and C-6). Mass: m/z (%) 268 (M^+, 17), 148 (100), 120 (93), 105 (19), 92 (58), 77 (80), 65 (36), 51 (37). Anal. Calcd. for $C_{14}H_{12}N_4O_2$: C, 62.68; H, 4.51; N, 20.88. Found: C, 63.02; H, 4.43; N, 21.05.

2-[2-(Pyridin-4ylmethylidene)hydrazinyl]-2-oxo-N-phenylacetamide ***(7n)***

m.p = 288-290 °C (EtOH), yield 91%, IR (KBr): νcm^{-1} 3303, 3255 (NH, stretch), 1697, 1661 (C=O, stretch). ^{1}H-NMR (250 MHz, DMSO-d_6): δppm 12.52 (s, 1H, NH), 10.78 (s, 1H, NH), 8.59 (d, *J* = 4.8 Hz, 2H, H_2', H_6'), 8.52 (s, 1H, N=CH), 7.76 (d, *J* = 7.8 Hz, 2H, H_2, H_6), 7.57 (d, *J* = 4.8 Hz, 2H, H_3', H_5'), 7.29 (t, *J* = 7.5 Hz, 2H, H_3, H_5), 7.07 (t, *J* = 7.3 Hz, 1H, H_4). ^{13}C-NMR (60 MHz, DMSO-d_6): δppm 158.5 (C=O), 157.3 (C=O), 150.8 (C-2' and C-6'),

149.1 (=C), 141.4 (C-4'), 137.9 (C-1), 129.2 (C-3 and C-5), 125.2 (C-4), 121.7 (C-3' and C-5'), 121.0 (C-2 and C-6). Mass: m/z (%) 268 (M^+, 56), 148 (100), 120 (59), 92 (56), 77 (71), 65 (30), 51 (35). Anal. Calcd. for $C_{14}H_{12}N_4O_2$: C, 62.68; H, 4.51; N, 20.88. Found: C, 62.57; H, 4.70; N, 21.15.

Antiproliferative activity

The synthesized compounds (**7a-7n**) were assessed individually for their anti-proliferative activity against a panel of cancer cell lines (MDA-MB-231, Hep-G2, HT-29, and MCF-7) at a concentration of 50 μM following 72 h of incubation. The antiproliferative activity was determined using MTT assay which is based on the ability of viable cells to reduce tetrazolium bromide to formazan. Our preliminary screening demonstrated that almost all compounds exerted a weak to moderate anti-proliferative activity towards the tested cell lines, decreasing cell viability to lower than about 50% (Table 1). Amongst them, compound **7k** displayed remarkable efficacy with cell growth inhibition of more than 90% in MDA-MB-231 and HepG2 cells. Doxorubicin was used as a standard drug. DMSO was applied as the vehicle, which showed no significant effect on the viability of the cells. The MDA-MB-231 cell line was selected for further evaluation because not only it exhibited a desirable sensitivity towards compound **7k**, but we could further verify our experiments in the established animal model of breast cancer. In the current study, IC_{50} values of compound **7k** were determined on MDA-MB-231 cells at 24, 48, and 72 h (Table 2). Since the animal model of breast cancer is established by inoculation of 4T1 cells into the mice, we also obtained the IC_{50} values of compound **7k** on 4T1 cells and reported them in Table 2. Furthermore, this compound revealed viability of more than 50% even at the highest concentration used towards normal cells confirming a suitable selectivity index (SI greater than 6.5; Fig. 2).

Table 1. Cell growth inhibition screening for compounds **7a-7n** following treatment at 50 μM for 72 h, towards human cancer cell lines. [a] Values were determined in at least three independent experiments each performed in triplicate and expressed as mean ± SEM.

Aryl	Compound	Cell growth inhibition (%)			
		MDA-MB-231	HepG2	HT-29	MCF7
phenyl	**7a**	25.57± 4.43	9.336 ± 1.16	8.527 ± 4.31	21.53 ± 1.31
2-chlorophenyl	**7b**	29.87 ± 2.63	49.17 ± 1.75	ND	23.54±1.89
3-chlorophenyl	**7c**	38.49 ± 3.23	48.89 ± 3.55	5.36 ± 1.53	11.60 ±3.66
4-chlorophenyl	**7d**	23.70 ± 0.94	44.52 ± 1.9	40.76 ± 1.06	5.301 ±3.5
2-bromophenyl	**7e**	38.07 ± 3.39	47.73 ± 1.78	ND	23.22 ± 2.23
3-bromophenyl	**7f**	25.84 ± 1.54	29.68 ± 4.55	13.16 ± 1.18	3.85 ± 3.52
4-bromophenyl	**7g**	23.21 ± 3.921	24.58 ± 6.77	45.02 ± 1.19	ND
2-nitrophenyl	**7h**	33.39 ± 2.68	45.09 ± 2.73	20.66 ± 1.63	9.22 ± 1.6
3-nitrophenyl	**7i**	13.25 ± 0.91	35.61 ± 0.84	15.52 ± 5.68	20.36 ± 1.95
4-nitrophenyl	**7j**	1.08 ± 1.8	45.98 ± 0.36	ND	19.02 ± 1.26
2-hydroxyphenyl	**7k**	92.02± 0.35	95.62 ± 0.58	50.79 ± 7.63	55.93 ± 1.71
2-pyridyl	**7l**	26.24 ± 1.58	28.47 ± 2.33	4.64 ± 2.4	19.26 ± 2.06
3-pyridyl	**7m**	25.54 ± 1.89	48.75 ± 3.42	0.83 ± 1.52	18.28 ± 2.08
4-pyridyl	**7n**	6.91 ± 1.43	24.69 ± 4.92	2.81 ± 1.07	16.08 ± 1.77
Vehicle	**-**	3.1 ± 1.14	2.71 ± 5.2	2.71 ± 0.7	8.95 ± 2.03
Doxorubicin	**-**	95.96 ± 0.23	90.16 ± 0.7	74.74 ± 0.58	ND

ND, Not determined.

Table 2. IC_{50} values for the antiproliferative activity of compound **7k** towards MDA-MB-231 and 4T1 cells. Values were determined in at least three independent experiments each performed in triplicate and expressed as mean ± SEM.

Cell lines	IC_{50} (μM) at 24 h	IC_{50} (μM) at 48 h	IC_{50} (μM) at 72 h
MDA-MB-231	35.86 ± 1.13	14.93 ± 1.05	7.73 ± 1.05
4T1	13.3 ± 1.07	5.09 ± 1.06	1.82 ± 1.14

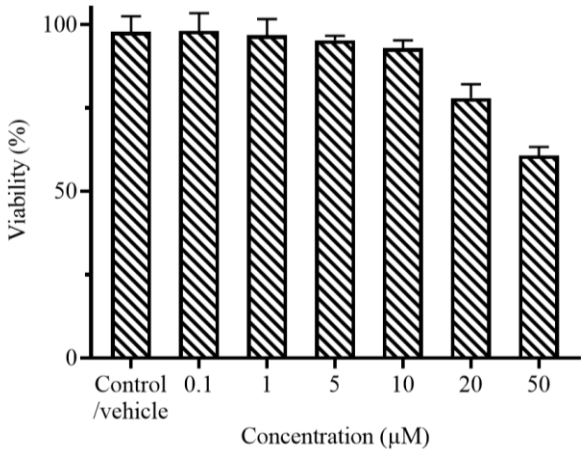

Fig. 2. The effect of compound **7k** at different concentrations on the viability of HSF cells, after 72-h treatment, using MTT assay.

Cell cycle arrest occurred by compound 7k

From the above-mentioned results, it was apparent that compound **7k** treatment caused significant cell death against both MDA-MB-231 and 4T1 cell lines. Thus, to unveil whether it was owing to the cell cycle arrest, an analysis of the cell cycle distribution was carried out. Data from Fig. 3 indicated that in the MDA-MB-231 untreated control cells, 57.9% of the cells were in G0/G1 phase while treatment with compound **7k** at 12 μM resulted in an increase in the cell population up to 67.75%. Notably, the percentage of the cells in this phase progressively augmented at higher concentrations (16 μM, 77.87%). In addition, following treatment with compound **7k**, the cell population in the S phase decreased from 32.1% in the control group to 27.3% and 19.6% in the treated cells with 12 μM and 16 μM, respectively. Arrest in the G1/S phase was remarkable at concentrations of 12 and 16 μM. For 4T1 cells, the ratio of the cells in the sub-G1 phase significantly increased from 7.33% in the control/vehicle to 24.36% in the treated group with 8 μM, while no significant increment was observed at other used concentrations. Concomitantly, the number of 4T1 cells in the S phase augmented from 36.18% in the control cells to 46.63% in the 8 μM-treated cells. Although the percentage of cells in the G2/M phase did not alter following treatment with an 8 μM concentration of compound **7k**, we speculate a probable S/G2 arrest (Fig. 4).

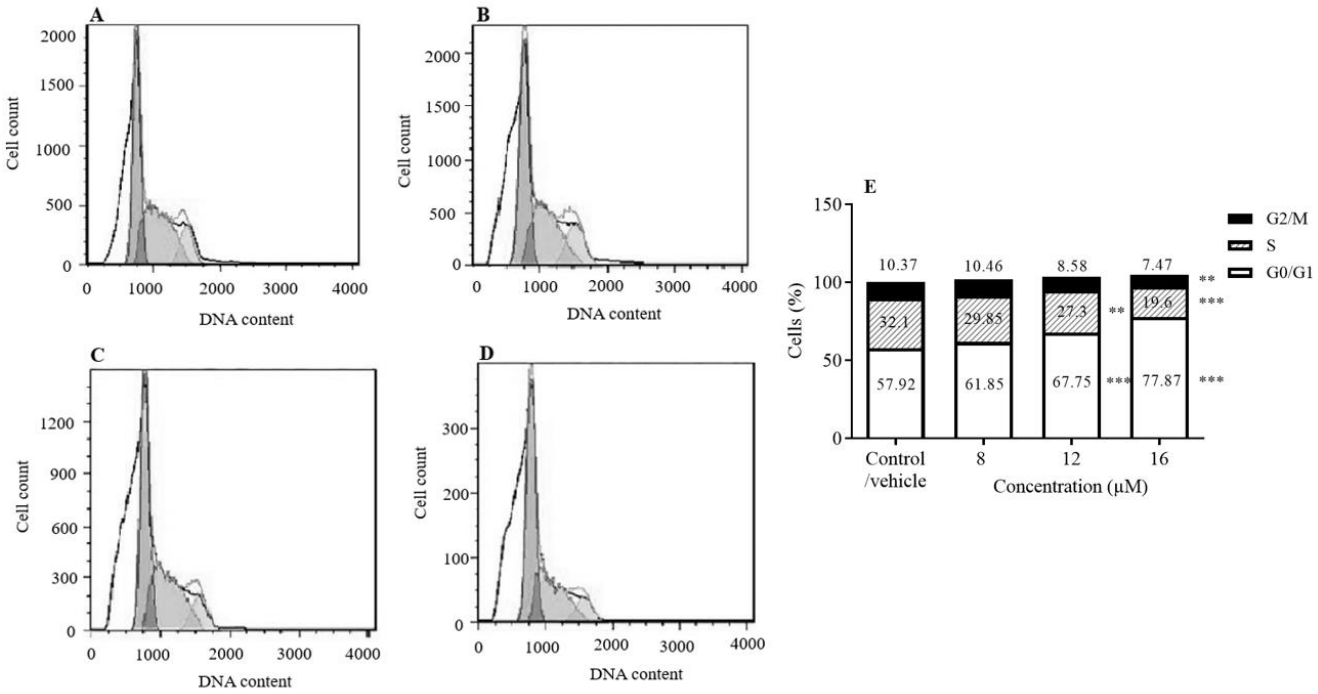

Fig. 3. Cell cycle distribution of (A) MDA-MB-231 cells and the cells treated with compound **7k** at (B) 8 μM, (C) 12 μM, and (D) 16 μM for 72 h in G0/G1, S, and G2/M phases using flow cytometry after staining with propidium iodide (PI). (E)The data presented in the graph are the mean ± SEM of three independent experiments. $^{**}P < 0.01$ and $^{***}P < 0.001$ indicate significant differences in comparison with the respective control/vehicle group.

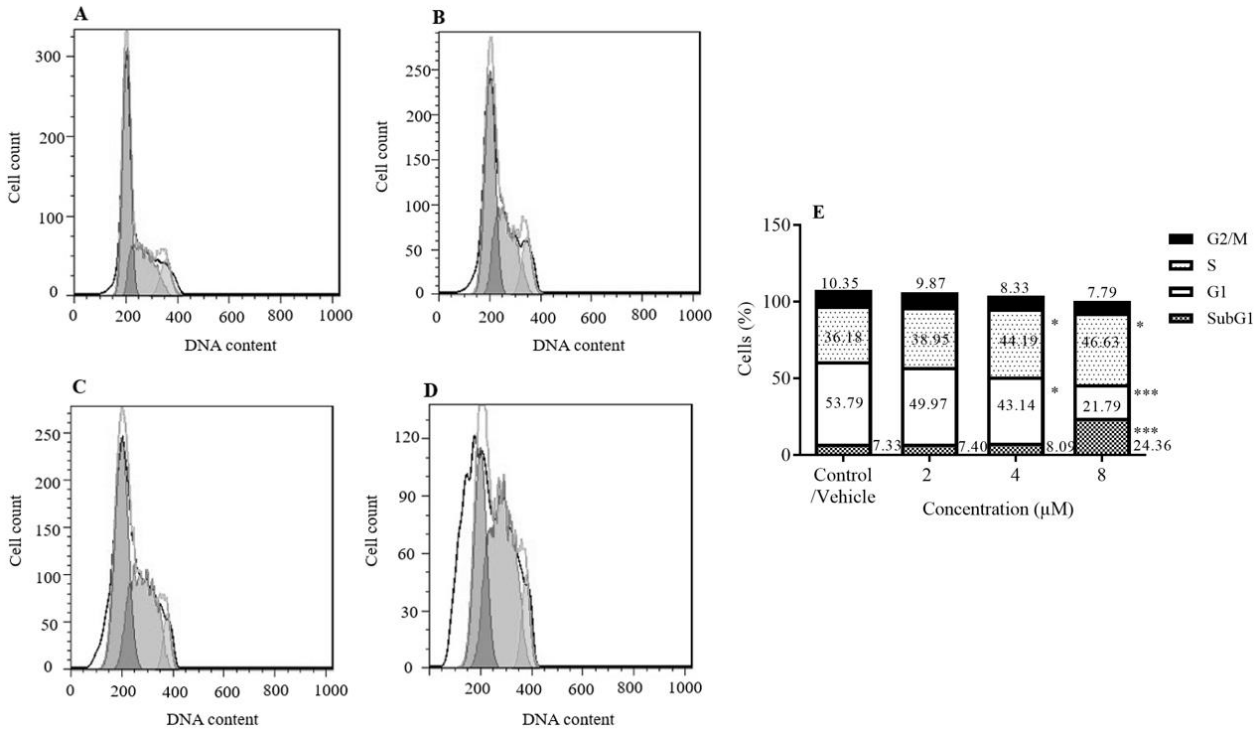

Fig. 4. Cell cycle distribution of (A) 4T1 cells and the cells treated with compound **7k** at (B) 2 µM, (C) 4 µM, and (D) 8 µM for 72 h in G0/G1, S, and G2/M phases using flow cytometry after staining with propidium iodide (PI). (E) The data presented in the graph are the mean ± SEM of three independent experiments. *$P < 0.05$ and ***$P < 0.001$ indicate significant differences in comparison with the respective control/vehicle group.

DISCUSSION

Currently, anticancer agents with different molecular mechanisms are applied in cancer treatment, though developing novel, effective, and promising agents are urgently required. In this context, the combination of hydrazone and α-ketoamide is expected to provide a novel design for the anticancer agents. Based on our literature survey, these hybrids have been linked to multiple biological functions such as anticancer effects (9,21-22). Hence, to ascertain our speculation, a series of compounds (**7a-7n**) were synthesized and investigated *in vitro* to achieve an efficacious compound possessing an antiproliferative effect.

Structures of the synthesized hybrid molecules were determined by spectral analysis data. In the FT-IR spectra, two NH absorptions over 3000 cm^{-1} were detected. Due to the similarity of the carbonyl groups; i.e., both are amide types, two carbonyl peaks were seen in most of the compounds as one broad absorbance between 1650-1700 cm^{-1} (31). In ^{1}H-NMR, two NH hydrogens were found at about 10.00 and 12.00 ppm and imine hydrogen was discovered close to 8.5 ppm implying the formation of an E isomer. In 13C-NMR, the carbonyl moieties were found in the range of 156-158 ppm and imine carbon was detected at about 147 to 151 ppm. At the outset of our project, we employed an MTT test on a panel of cancer cells to drive our optimization effort. Our preliminary screening returned compound **7k** as a potent anti-proliferative agent. It showed proliferation inhibition of more than 90% at 72 h against the Hep-G2 and MDA-MB-231 cells at 50 µM as an initial concentration to elude the false-negative and false-positive effects at the lower and higher concentrations. By contrast, HT-29 and MCF-7 cell lines were substantially less sensitive to this compound. Interestingly, this compound demonstrated reasonable viability toward normal cells. To present a detailed structure-activity description, we introduced a number of substituents at various positions at the aromatic ring attached to the hydrazone moiety in order to improve the potency. Comparison of compound **7a** with **7b**, **7e,** and **7h** showed that insertion of electron-withdrawing groups at position 2 of the phenyl ring resulted in increasing the activity. The

introduction of Cl at the *meta* position improves the activity but no advantage was observed by replacing it with Br. However, employing the polar and strong electron-accepting groups at the *meta* position led to a significant decrease in cell viability. The existence of electron-accepting moieties like Cl, Br, and NO_2 at position 4 of the phenyl ring demonstrated a deteriorative effect on the potency. Furthermore, the bioisosteric replacement of phenyl with the pyridyl substituents gave rise to the formation of compounds **7l** and **7m** with negligible changes in potency and **7n** with a dramatic reduction in activity when compared to **7a**. Interestingly, compounds **7j** and **7n** bearing 4-nitrophenyl and 4-pyridyl and as bioisosteres exhibited the weakest potency in cell proliferation. These findings are in contrast to other studies indicating that the replacement of phenyl ring with heteroaryl groups like pyridine in hydrazone derivatives increased the antitumor potential (32). Surprisingly, the presence of a strong polar electron donating group at position 2 led to compound **7k** as the most active derivative. Overall, electron density at the phenyl ring of the hydrazone group or H-bond donating ability decreased the proliferative activity of the compounds. This conclusion is in agreement with the reports of Wu *et al.* and Cui *et al.* implying the anticancer-enhancing effect of 2-hydroxyl phenyl moiety in N-acyl hydrazone derivatives (33,34). Thus, we determined the IC_{50} value of this compound on MDA-MB-231 cells at 24, 48, and 72 h due to the concentration-dependent effect of the compound. It is noteworthy that a significant cell growth inhibition was also shown for compound **7k** on 4T1 cells. These data not only verified the IC_{50} values on MDA-MB-231 cells but also provided a suitable background for our ongoing *in vivo* studies.

Seeking to understand the role of cell cycle arrest as an appealing approach in cancer therapy, we applied flow cytometry analysis to evaluate the mechanism of action of cell death induced by compound **7k**. MDA-MB-231 cell subpopulations behaved differently based on the concentration of the compound. The histogram of 8 μM-treated cells was the same as that of the vehicle-treated cells, while treatment with 12 and 16 μM led to an increase in cell subpopulation at G1-phase and a decrease at S-phase, in comparison with vehicle-treated cells suggesting a G1/S arrest. Therefore, we propose that cell death induced by compound **7k** is an event linked to cell cycle arrest.

CONCLUSION

Altogether, we herein report the percentage of proliferation inhibition of a new series bearing oxamide and hydrazone moieties (**7a-7n**) towards human cancer cell lines, among which compound **7k** possessing 2-hydroxyphenyl moiety showed the greatest anti-proliferative effect against MDA-MB-231 cells at 72 h. Also, we suggest that cell death is also correlated with G1/S cell cycle arrest. Interestingly, this synthesized compound exhibited a concentration-dependent mode of action, making it likely to have great potency to treat cancer cells.

Acknowledgments

This research received no specific grant from any funding agency in the public, commercial, or not-for-profit sectors.

Conflict of interest statement

The authors declared no conflicts of interest in this study.

Authors' contributions

M. Dehbid and R. Tahmasvand contributed to the biological experiments and data collection. M. Tasharofi and F. Shojaie synthesized the compounds. M. Aghamaali contributed to analyzing the data. A. Almasirad designed the structures, supervised the synthesis of the compounds and interprete the spectra of the compounds. M. Salimi wrote the manuscript, provided technical support, and supervised the whole project. The final version of the manuscript was approved by all authors.

REFERENCES

1. Ma X, Yu H. Global burden of cancer. Yale J Biol Med. 2006;79(3-4): 85-94. PMID: 17940618.
2. DeSantis CE, Ma J, Gaudet MM, Newman LA, Miller KD, Sauer AG, *et al*. Breast cancer statistics. CA Cancer J Clin. 2019;69(6):438-451. DOI: 10.3322/caac.21583.

3. Dent R, Trudeau M, Pritchard KI, Hanna WM, Kahn HK, Sawka CA, *et al*. Triple-negative breast cancer: clinical features and patterns of recurrence. Clin Cancer Res. 2007;13(15 Pt 1):4429-4434. DOI: 10.1158/1078-0432.CCR-06-3045.
4. Almansour NM. Triple-negative breast cancer: a brief review about epidemiology, risk factors, signaling pathways, treatment and role of artificial intelligence. Front Mol Biosci. 2022;9: 36417. DOI: 10.3389/fmolb.2022.836417.
5. Pernas S, Tolaney SM. HER2-positive breast cancer: new therapeutic frontiers and overcoming resistance. Ther Adv Med Oncol. 2019;11:1-16. DOI: 10.1177/1758835919833519.
6. Rollas S and Küçükgüzel SG. Biological activities of hydrazone derivatives. Molecules. 2007;12(8):1910-1939. DOI: 10.3390/12081910.
7. Şenkardeş S, Han MI, Kulabaş N, Abbak M, Çevik Ö, Küçükgüzel I, *et al*. Synthesis, molecular docking and evaluation of novel sulfonyl hydrazones as anticancer agents and COX-2 inhibitors. Mol Divers. 2020;24(3):673-689. DOI: 10.1007/s11030-019-09974-z.
8. Sreenivasulu R, Reddy KT, Sujitha P, Kumar CG, Raju RR. Synthesis, antiproliferative and apoptosis induction potential activities of novel bis (indolyl) hydrazide-hydrazone derivatives. Bioorg Med Chem. 2019;27(6):1043-1055. DOI: 10.1016/j.bmc.2019.02.002.
9. Mousavi E, Tavakolfar S, Almasirad A, Kooshafar Z, Dehghani S, Afsharinasab A, *et al*. *In vitro* and *in vivo* assessments of two novel hydrazide compounds against breast cancer as well as mammary tumor cells. Cancer Chemother Pharmacol. 2017;79(6):1195-1203. DOI: 10.1007/s00280-017-3318-5.
10. Nam DH, Lee KS, Kim SH, Kim SM, Jung SY, Chung SH, *et al*. Design and synthesis of 4-quinolinone 2-carboxamides as calpain inhibitors. Bioorg Med Chem Lett. 2008;8(1):205-209. DOI: 10.1016/j.bmcl.2007.10.097
11. Zulkepli NA, Rou KVK, Sulaiman WNHW, Salhin A, Saad B, Seeni A. A synthetic hydrazone derivative acts as an apoptotic inducer with chemopreventive activity on a tongue cancer cell line. Asian Pac J Cancer Prev. 2011;12(1):259-263. PMID: 21517268.
12. Zheng LW, Wu LL, Zhao BX, Dong WL, Miao JY. Synthesis of novel substituted pyrazole-5-carbohydrazide hydrazone derivatives and discovery of a potent apoptosis inducer in A549 lung cancer cells. Bioorg Med Chem. 2009;17(5):1957-1962. DOI: 10.1016/j.bmc.2009.01.037.
13. do Amaral DN, Cavalcanti BC, Bezerra DP, Ferreira PMP, Castro RDP, Sabino JR, *et al*. Docking, synthesis and antiproliferative activity of N-acylhydrazone derivatives designed as combretastatin A_4 analogues. PLoS One. 2014;9(3):e85380. DOI: 10.1371/journal.pone.0085380.
14. Takao H, Takeda Y, Haginoya N, Miyazaki M, Nagata M, Kitagawa M, *et al*. Discovery of novel thieno [2, 3-d] pyrimidin-4-yl hydrazone-based cyclin-dependent kinase 4 inhibitors: synthesis, biological evaluation and structure-activity relationships. Chem Pharm Bull (Tokyo). 2011;59(8):991-1002. DOI: 10.1248/cpb.59.991.
15. Fan C, Su H, Zhao J, Zhao B, Zhang S, Miao J. A novel copper complex of salicylaldehyde pyrazole hydrazone induces apoptosis through up-regulating integrin β4 in H322 lung carcinoma cells. Eur J Med Chem. 2010;45(4):1438-1446. DOI: 10.1016/j.ejmech.2009.12.048.
16. Effenberger K, Breyer S, Schobert R. Modulation of doxorubicin activity in cancer cells by conjugation with fatty acyl and terpenyl hydrazones. Eu J Med Chem. 2010;45(5):1947-1954. DOI: 10.1016/j.ejmech.2010.01.037.
17. Nasr T, Bondock S, Rashed HM, Fayad W, Youns M, Sakr TM. Novel hydrazide-hydrazone and amide substituted coumarin derivatives: synthesis, cytotoxicity screening, microarray, radiolabeling and *in vivo* pharmacokinetic studies. Eur J Med Chem. 2018;151:723-739. DOI: 10.1016/j.ejmech.2018.04.014.
18. Zhao Y, Hui J, Wang D, Zhu L, Fang JH, Zhao XD. Synthesis, cytotoxicity and pro-apoptosis of novel benzoisoindolin hydrazones as anticancer agents. Chem Pharm Bull (Tokyo). 2010;58(10):1324-1327. DOI: 10.1248/cpb.58.1324.
19. Rodrigues DA, Guerra FS, Sagrillo FS, Pinheiro PDSM, Alves MA, Thota S, *et al*. Design, synthesis, and pharmacological evaluation of first-in-class multitarget N-acylhydrazone derivatives as selective HDAC6/8 and PI3Kα inhibitors. Chem Med Chem. 2020;15(6);539-551. DOI: 10.1002/cmdc.201900716.
20. Wada CK, Frey RR, Ji Z, Curtin ML, Garland RB, Holms JH, *et al.* α-Keto amides as inhibitors of histone deacetylase. Bioorg Med Chem Lett. 2003;13:3331-3335. DOI: 10.1016/s0960-894x(03)00685-1.
21. Lee KY, Lee KS, Jin C, Lee YS. Design and synthesis of calpain inhibitory 6-pyridone 2-carboxamide derivatives. Eur J Med Chem. 2009;44(3):1331-1334. DOI: 10.1016/j.ejmech.2008.02.023.
22. Tavakolfar S, Mousavi E, Almasirad A, Amanzadeh A, Atyabi SM, Yaghamii P, *et al*. *In vitro* anticancer effects of two new potent hydrazide compounds on leukemic cells. Anticancer Agents Med Chem. 2016;16(12):1646-1651. DOI: 10.2174/1871520616666160404112945.
23. Wang C, Li y, Liu T, Wang Z, Zhang Y, Bao K, *et al*. Design, synthesis and evaluation of antiproliferative and antitubulin activities of 5-methyl-4-aryl-3-(4-arylpiperazine-1-carbonyl)-4H-1, 2, 4-triazoles. Bioorg Chem. 2020;104:103909. DOI: 10.1016/j.bioorg.2020.103909.
24. Yousef T, El-Reash GA, Rakha T, El-Ayaan U. First row transition metal complexes of (E)-2-(2-(2-hydroxybenzylidene) hydrazinyl)-2-oxo-N-phenylacetamide complexes. Spectrochim Acta A Mol Biomol Spectrosc. 2011;83(1):271-278.

DOI: 10.1016/j.saa.2011.08.030.
25. Zakalyuzhnyi M, Zakalyuzhnyi YM, Pershin G, Zykova T, Gus' kova T. Benzylidene-and nitrobenzylideneoxanyloyl-hydrazide and their antimicrobial activity. Pharm Chem J. 1973;7: 679-681.
DOI: 10.1007/BF00757931.
26. Cremlyn RJ. Synthesis and spectral data for some derivatives of N-aryloxamic acid hydrazides. J Chem Eng Data.1974;19:288-294.
DOI: 10.1021/je60062a005.
27. El-Gammal OA, El-Reash GA, Ahmed S. Synthesis, spectral characterization, molecular modeling and *in vitro* antibacterial activity of complexes designed from O_2, NO and NO donor Schiff-base ligand. Spectrochim Acta A Mol Biomol Spectrosc. 2015;135:227-240.
DOI: 10.1016/j.saa.2014.04.197.
28. Tierie G. Oxanilhydrazides. Rec Trav Chim. 1993;52(6):533-537.
DOI: 10.1002/recl.19770960402.
29. Shah R. Ligational, potentiometric and floatation studies on Cu (II) complexes of hydrazones derived from p and o-vanillin condensed with diketo hydrazide. J Mol Liq. 2016;220:939-953.
DOI: 10.1016/j.molliq.2016.04.047
30. Tahmasvand R, Bayat P, Vahdaniparast SM, Dehghani S, KooshafarZ, Khaleghi S, *et al*. Design and synthesis of novel 4-thiazolidinone derivatives with promising anti-breast cancer activity: synthesis, characterization, *in vitro* and *in vivo* results. Bioorg Chem. 2020;104:104276,1-13.
DOI: 10.1016/j.bioorg.2020.104276.
31. Asadi M, Mohammadi-Khanaposhtani M, Hosseini FS, Gholami M, Dehpour AR, Amanlou M. Design, synthesis, and evaluation of novel racecadotril-tetrazole-amino acid derivatives as new potent analgesic agents. Res Pharm Sci. 2021;16(4):341-357.
DOI: 10.4103/1735-5362.319573.
32. Mohareb RM, Fleita DH, Sakka OL. Novel synthesis of hydrazide-hydrazone derivatives and their utilization in the synthesis of coumarin, pyridine, thiazole and thiophene derivatives with antitumor activity. Molecules. 2011;16(1):16-27.
DOI: 10.3390/molecules16010016.
33. Wu J, Zhang D, Chen L, Li J, Wang J, Ning C, *et al*. Discovery and mechanism study of SIRT1 activators that promote the deacetylation of fluorophore-labeled substrate. J Med Chem. 2013,56(3),761-780.
DOI: 10.1021/jm301032j.
34. Cui Z, Li Y, Ling Y, Huang J, Cui J, Wang R, *et al*. New class of potent antitumor acylhydrazone derivatives containing furan. Eur J Med Chem. 2010;45(12):5576-5584.
DOI: 10.1016/j.ejmech.2010.09.007.